The EMBO Journal Vol.18 No.22 pp.6329–6338, 1999

Ca^{2+} bridges the C2 membrane-binding domain of protein kinase Cα directly to phosphatidylserine

Nuria Verdaguer, Senena Corbalan-Garcia[1], Wendy F.Ochoa, Ignacio Fita and Juan C.Gómez-Fernández[1,2]

IBMB-CSIC, Jordi Girona Salgado 18,26, E-08034 Barcelona and [1]Departamento de Bioquímica y Biología Molecular (A), Facultad de Veterinaria, Universidad de Murcia, Apartado de Correos 4021, E-30080 Murcia, Spain

[2]Corresponding author
e-mail: jcgomez@fcu.um.es

N.Verdaguer and S.Corbalan-Garcia contributed equally to this work

The C2 domain acts as a membrane-targeting module in a diverse group of proteins including classical protein kinase Cs (PKCs), where it plays an essential role in activation via calcium-dependent interactions with phosphatidylserine. The three-dimensional structures of the Ca^{2+}-bound forms of the PKCα-C2 domain both in the absence and presence of 1,2-dicaproyl-*sn*-phosphatidyl-L-serine have now been determined by X-ray crystallography at 2.4 and 2.6 Å resolution, respectively. In the structure of the C2 ternary complex, the glycerophosphoserine moiety of the phospholipid adopts a quasi-cyclic conformation, with the phosphoryl group directly coordinated to one of the Ca^{2+} ions. Specific recognition of the phosphatidylserine is reinforced by additional hydrogen bonds and hydrophobic interactions with protein residues in the vicinity of the Ca^{2+} binding region. The central feature of the PKCα-C2 domain structure is an eight-stranded, antiparallel β-barrel with a molecular topology and organization of the Ca^{2+} binding region closely related to that found in PKCβ-C2, although only two Ca^{2+} ions have been located bound to the PKCα-C2 domain. The structural information provided by these results suggests a membrane binding mechanism of the PKCα-C2 domain in which calcium ions directly mediate the phosphatidylserine recognition while the calcium binding region 3 might penetrate into the phospholipid bilayer.

Keywords: Ca^{2+} binding/C2 domain/phosphatidylserine/protein kinase C/X-ray structure

Introduction

Protein kinase C (PKC) refers to a large diversity of phospholipid-dependent serine/threonine kinases that can be activated upon external stimulation of cells by a number of ligands including growth factors, hormones and neurotransmitters (Basu, 1993; Newton, 1995; Nishizuka, 1995; Mellor and Parker, 1998). PKC in mammalian cells consists of at least 11 closely related isoenzymes that, in general, contain four conserved domains named C1–C4 (Coussens *et al*., 1986). According to their structure and cofactor regulation, PKCs can be classified into three groups. The first group, which includes the classical isoforms (α, βI, βII and γ), can be distinguished from the other groups because functioning is regulated by diacylglycerol (DAG) and also cooperatively by calcium and acidic phospholipids, particularly phosphatidylserine (PS). Members of the second group are the novel mammalian (δ, ε, η and θ) and yeast PKCs that are not regulated by calcium and present a molecular organization similar to the classical isoforms except for differences in the C2 domain. The third group comprises the atypical PKC isoforms (ζ, λ and μ), which lack the C2 domain and are regulated neither by DAG nor by calcium (Dekker and Parker, 1994; Newton and Johnson, 1998).

In the classical PKCα isoenzyme, the Ca^{2+}-dependent binding to membranes presents a high specificity for 1,2-*sn*-phosphatidyl-L-serine (Boni and Rando, 1985; Lee and Bell, 1989; Newton and Keranen, 1994; Johnson *et al*., 1998). Furthermore, it has also been shown that this binding is mediated by the C2 domain both *in vitro* and *in vivo* (Edwards and Newton, 1997; Medkova and Cho, 1998; Corbalan-Garcia *et al.*, 1999). Homologs of the PKCα-C2 domain correspond to regulatory sequence motifs of ~130 amino acids, existing in a large variety of proteins involved in intracellular signaling and membrane trafficking (Nalefski and Falke, 1996; Rizo and Südhof, 1998). Crystal structures of C2 domains from synaptotagmin I (Sutton *et al.*, 1995), phospholipase C-δ (Essen *et al.*, 1996), phospholipase A_2 (Perisic *et al.*, 1998; Bittova *et al.*, 1999; Dessen *et al.*, 1999), PKCβ (Sutton and Sprang, 1998) and PKCδ (Pappa *et al.*, 1998) have revealed a homologous β-sandwich fold that serves in the first four proteins as the scaffold for a generally bipartite Ca^{2+} binding site formed by a pair of loops that project from the opposing β-sheets. The C2 domains of synaptotagmin and the two phospholipases adopt alternative type I and type II connectivities that differ by circular permutation of their topologies (reviewed by Nalefski and Falke, 1996; Rizo and Sudhof, 1998). C2 domains of classical PKCs can be classified as having a type I topology (Sutton and Sprang, 1998), while in the novel PKCδ the C2 domain has been found to exhibit a type II topology similar to that of the phospholipases but with a degenerated Ca^{2+} binding site (Pappa *et al*., 1998).

Mechanisms involved in the membrane interactions with the C2 domain remain unclear and neither the structural basis for cooperativity between lipids and Ca^{2+} nor the lipid specificity are well understood for PKCs. The structural information on the PKCα-C2 domain complexes obtained in the present work suggests a membrane binding mechanism in which one calcium ion directly mediates the PS-specific recognition, while the calcium binding region 3 (CBR3) might penetrate into the phospholipid

Table I. Data collection and refinement statistics of PKCα-C2–Ca^{2+} and PKCα-C2–Ca^{2+}–DCPS structures

Parameters	PKCα-C2–Ca^{2+}–DCPS		PKCα-C2–Ca^{2+}
Space group	$P3_221$		$P3_221$
Cell dimensions (Å)	$a = b = 58.81$, $c = 91.68$		$a = b = 58.35$, $c = 91.62$
Resolution (Å)	2.6		2.4
Reflections			
Total	17 072		11 214
Unique	5610		6553
R_{symm} (%)	9.2		5.5
Completeness (%)	94.3		88.9
Refinement reflections	5432		6292
Resolution range (Å)	18–2.6		20–2.4
Non-H atoms	1110		1106
Solvent molecules	38		76
Counterions	3 (2 Ca^{2+}; 1 PO_4^{3-})		4 (2 Ca^{2+}; 2 PO_4^{3-})
Mean *B*-factor (Å^2)			
Protein	25.6		28.2
Water molecules	32.6		36.7
Calcium ions	24.5		32.3
Phosphate ions	41.5		37.2
DCPS ligand	40.8		–
R.m.s. deviations from standard			
Bond lengths (Å)	0.015		0.018
Bond angles (°)	1.4		1.6
	sn-1 model	*sn*-2 model	
R_{work} (%)	19.5	19.6	22.7
R_{free} (%)	23.3	23.6	27.1

bilayer. This translocation mechanism appears to be in agreement with data about lipid specificity, cooperativity with calcium ions and most observations derived from mutational studies.

Results

Overall structures

Crystals of the calcium bound forms of the PKCα-C2 domain, including from His155 to Gly293 residues, were obtained and analyzed by X-ray crystallography both in the absence (PKCα-C2–Ca^{2+}) and in the presence of the short chain lipid 1,2-dicaproyl-*sn*-phosphatidyl-L-serine (DCPS) (PKCα-C2–Ca^{2+}–DCPS). In the two crystal forms the quality of the final electron density map allowed the accurate positioning of most residues and side chains from the C2 domain. Only densities corresponding to the highly exposed N-terminal residues, His155 to Lys158, and to the side chains from Lys197, Lys199 and Arg252, were poorly defined in the two structures. The root mean square (r.m.s.) deviation of the superimposition of the C_α atoms from the two PKCα-C2 crystal structures determined is 0.22 Å, a value resulting from both model inaccuracies and real conformational differences that can be considered an upper limit error for the coordinates in the two structures. The high structural similarity between the protein conformation in the binary and ternary complexes extends to the disposition of most side chains, indicating that no important rearrangements of the C2 conformation were induced by the phospholipid binding. The PKCα-C2–Ca^{2+} structure, at 2.4 Å resolution, also shows 76 well ordered solvent molecules, two Ca^{2+} and two phosphate ions (Table I). The ternary complex PKCα-C2–Ca^{2+}–DCPS, determined at 2.6 Å resolution, includes 38 solvent molecules, two Ca^{2+}, one phosphate ion and one DCPS molecule with a partial occupancy >50%. Electron density corresponding to the DCPS ligand was well defined for the glycerophosphoserine head group moiety, but weakened towards the phospholipid acyl chains. The position corresponding to the phosphoryl group of the DCPS ligand was partially occupied in the binary complex by a phosphate ion from the solution employed for crystallization. A strong peak of extra density, both in the unbound and DCPS-bound structures, also suggested the presence of a phosphate ion at a conserved positively charged cluster (Sutton and Sprang, 1998), which in PKCα involves lysine residues 197, 199, 211 and 213 from strands β3 and β4.

The central structural feature of the PKCα-C2 domain is an eight-stranded, anti-parallel β-sandwich with the type I or S-type fold, which is a topology similar to the first C2 domain of synaptotagmin I (Figure 1) (Sutton *et al*., 1995). The PKCα-C2–Ca^{2+} domain structure retains most of the features found in the C2 domain of PKCβ including the organization of the Ca^{2+} binding region, as anticipated from the ~80% sequence identity between the two domains (Sutton and Sprang, 1998). The r.m.s. calculated between the equivalent C_α atoms of PKCα-C2 and PKCβ was only 0.43 Å for 130 equivalent residues. The r.m.s. deviation between equivalent C_α atoms of PKCα-C2 and synaptotagmin-C2A (type I fold) was 0.91 Å for 108 equivalent residues, whereas deviations from the type II fold PLC-δ-C2 (Essen *et al*., 1996), PLA2 (Perisic *et al*., 1998) and PKC-δ-C2 (Pappa *et al*., 1998) were 0.95, 0.82 and 1.40 Å for 87, 79 and 40 equivalent residues, respectively. The greatest variability among all these C2 domain structures is found in the N-terminal region and in the strand connections. The Ca^{2+} binding region 1 (CBR1), which corresponds to the β2–β3 connection, is similar in PKCα and β, while both present large

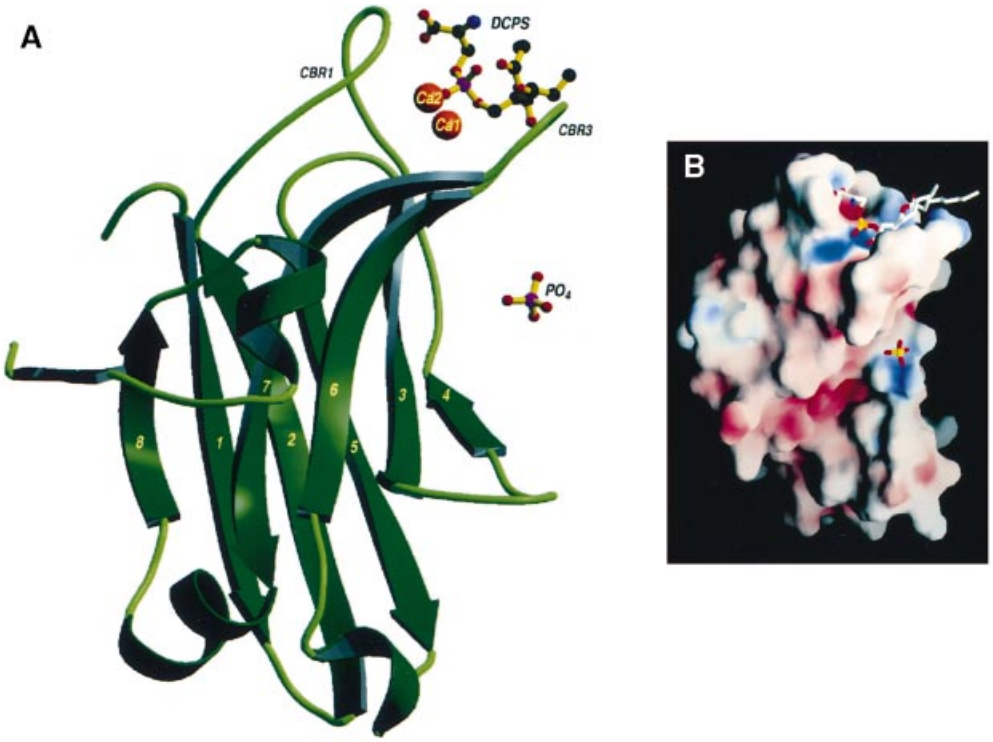

Fig. 1. (**A**) Overall structure of the C2 domain of PKCα bound to PS. β-strands are depicted as arrows numbered sequentially. The two Ca^{2+} ions located in the calcium binding site are also shown as orange spheres. The DCPS and phosphate molecules found in the ternary complex are explicitly shown as balls and sticks. (**B**) Surface potential drawing of the PKCα-C2–Ca^{2+} domain structure as computed and displayed by GRASP (Nicholls *et al*., 1991). Positively and negatively charged regions are shown in blue and red, respectively. The DCPS- and phosphate-bound molecules are also depicted as stick models.

differences to other C2 domain structures. In contrast, the organization of connection β6–β7, referred to as loop 3 or CBR3, is highly conserved among all the C2 domain structures. The comparison of the β3–β4 link of PKCα and β shows deviations >3 Å for the C_α atoms of equivalent residues. Finally the β7–β8 connection, located at the end of the β-sandwich opposite to the Ca^{2+} binding site, is a helix in PKCα and β but a loop in the remaining C2 structures available.

Ca^{2+} binding pocket

The two Ca^{2+} ions found in the PKCα-C2 structures (named Ca1 and Ca2 in Figures 1 and 2) are equivalent to the central calcium subsites (sites II and III, respectively) in PKCβ-C2 (Sutton and Sprang, 1998). However, the location corresponding to the third PKCβ-C2 Ca^{2+} binding subsite (site IV) is occupied by a water molecule in PKCα-C2. Ca1 and Ca2 ions in PKCα-C2 are related to each other by a pseudo-dyad symmetry axis, similar to what had been observed in most C2 structures (Shao *et al*., 1996; Essen *et al*., 1997). Protein ligands provide six of the seven oxygens that coordinate with each of the two Ca^{2+} ions and are located in loops β2–β3 (CBR1) and β6–β7 (CBR3) at distances ranging from 2.3 to 2.6 Å (Essen *et al*., 1997). These protein ligands correspond to the side chains of the five aspartate residues (187, 193, 246, 248, 254) and to the main chain of residues Met186 and Trp247 (Figure 2). Three aspartate ligands (187, 246 and 248) coordinate simultaneously with the two calcium ions. Asp246, situated on the pseudo-dyad axis, contributes one carboxylate oxygen to each of the Ca^{2+} ions. Asp187, related by the pseudo-dyad axis to Asp248, shows a bidentate interaction with Ca1, while still participating in one coordination bond with Ca2 (Figure 2C). On the other hand, Asp248 presents a bidentate interaction with Ca2 and a single coordination with Ca1.

The nature and disposition of the seventh ligand of the two Ca^{2+} ions depart completely from the pseudo-symmetric organization of the calcium binding pocket of the C2 domain. Ca1 is bound to the phosphoryl group of DCPS in the PKCα-C2–Ca^{2+}–DCPS ternary complex and is coordinated to a phosphate ion in the binary complex (Figure 2A and B). In turn, the seventh ligand of Ca2 is a water molecule in both the binary and ternary complexes (Figure 2). The organization of these ligands in PKCα differs from that found in PKCβ, where the seventh coordination position was empty for Ca1 and occupied by the side chain of a glutamic residue from a neighbor molecule for Ca2 (Sutton and Sprang, 1998).

Conformation and interactions of the DCPS ligand

In order to obtain the ternary complex of PKCα-C2 domain with PS and Ca^{2+} we have used DCPS, which has the peculiarity of being hydrosoluble at the 2 mM concentration used during the preparation of the PKCα-C2–Ca^{2+}–DCPS complex in this work, and it shows a critical micellar concentration of 29 mM (Walker *et al*., 1990). The presence of one bound molecule of DCPS in the crystal structure of the PKCα-C2–Ca^{2+}–DCPS complex was initially suggested by the prominent extra density,

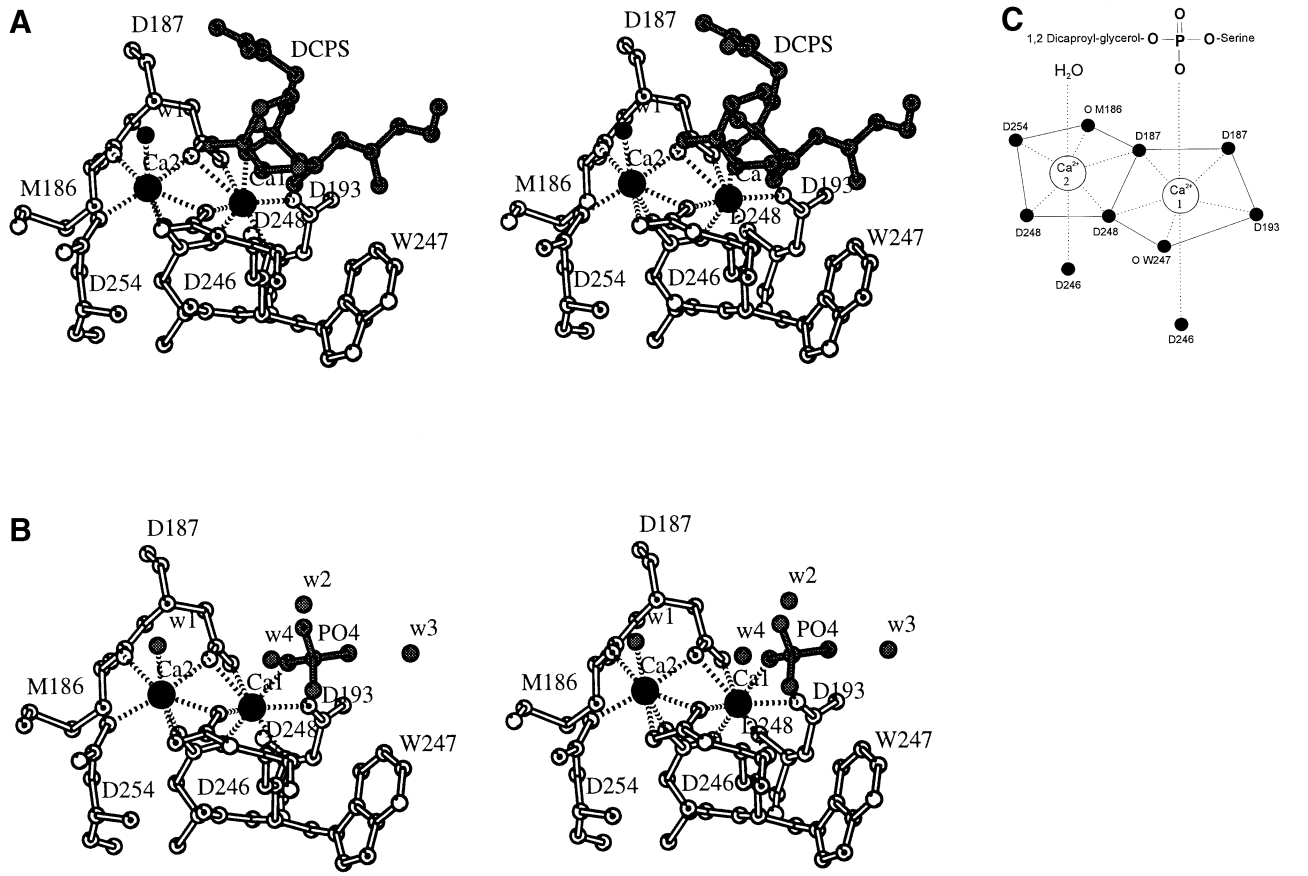

Fig. 2. Stereoview of the Ca^{2+} binding site of the PKCα-C2–Ca^{2+}–DCPS ternary complex (**A**) and of the PKCα-C2–Ca^{2+} binary complex (**B**). For both structures the seven coordination bonds of each calcium ion are represented as broken lines. Protein residues are shown in white, while the DCPS and phosphate ligands from the ternary and binary complexes, respectively, are shown in gray. Ca^{2+} ions and water molecules are depicted as large and smaller black balls, respectively. (**C**) Pseudosymmetric coordination scheme of the two Ca^{2+} ions found in the structure of the ternary complex.

with a nearly cyclic shape, located in the vicinity of Ca1 in difference Fourier maps (Figure 3). This density was interpreted as corresponding to the cyclization of the glycerophosphoserine backbone with a water molecule (named w0 in Figure 4). Two energetically feasible conformations of the phospholipid can be proposed from the electron density maps, as the similarity of the atomic dispositions retains the most significant peculiarities in the two alternative models even when taking into account protein–lipid interactions or stereochemical constraints (Figures 3C and 4). In the first conformation, the N-terminal group of the phosphoserine bridges to the fatty acyl *sn*-1 ester carbonyl group (model *sn*-1) throughout water molecule w0, which also interacts with a phosphoryl oxygen. In the alternative DCPS model (model *sn*-2), the bridging of the phosphoserine N-terminal group is with the ester carbonyl group of the fatty acyl *sn*-2 also throughout the water molecule w0. Model *sn*-1 (used in the representations of Figures 1, 2 and 5) behaved marginally better during the final cycles of crystallographic refinement (Table I). In the two models at least one of the oxygen atoms from the DCPS phosphoryl group coordinates directly with Ca1, while the seryl moiety interacts specifically with main and side chain nitrogen atoms of Asn189 from CBR1. Furthermore, in the two models, the DCPS fatty acyl chains present hydrophobic interactions with the aliphatic carbons from the CBR3 residue Arg249. Model *sn*-1 also shows hydrogen bonds of the *sn*-1 ester oxygen atom with the Arg249 main chain nitrogen. The fatty acyl *sn*-2 ester carbonyl group interacts with the guanidinium groups of Arg216 and Arg249 (Figure 4A). In this model, Thr251 was also found to interact with the fatty acyl *sn*-1 ester carbonyl group. Model *sn*-2 keeps some of the protein–lipid interactions with Arg216 interacting with the fatty acyl *sn*-1 ester carbonyl group and Thr251 with the *sn*-2 ester carbonyl group (Figure 4B).

The configuration and the interactions seen in the ternary complex provide likely explanations for the observed stereospecific selectivity of PKCα to 1,2-*sn*-phosphatidyl-L-serine (Newton and Johnson, 1998). Thus, attempts to model 2,3-*sn*-phosphatidyl-L-serine introduce steric clashes within the lipid binding pocket, while 1,2-*sn*-phosphatidyl-D-serine can not reproduce the interactions of the lipid with L-serine. The favorable character of the interaction between the phosphoryl group and Ca1 in the ternary complex is supported by the presence of a phosphate ion, though with partial occupancy, in the binary complex. This electrostatic interaction might also contribute to the binding of other anionic lipids. The presence of the phosphate ion in the binary complex also suggests that a percentage of the binding sites unoccupied by DCPS in the crystal of the ternary complex might be filled by phosphate with an occupancy of ~25% at most.

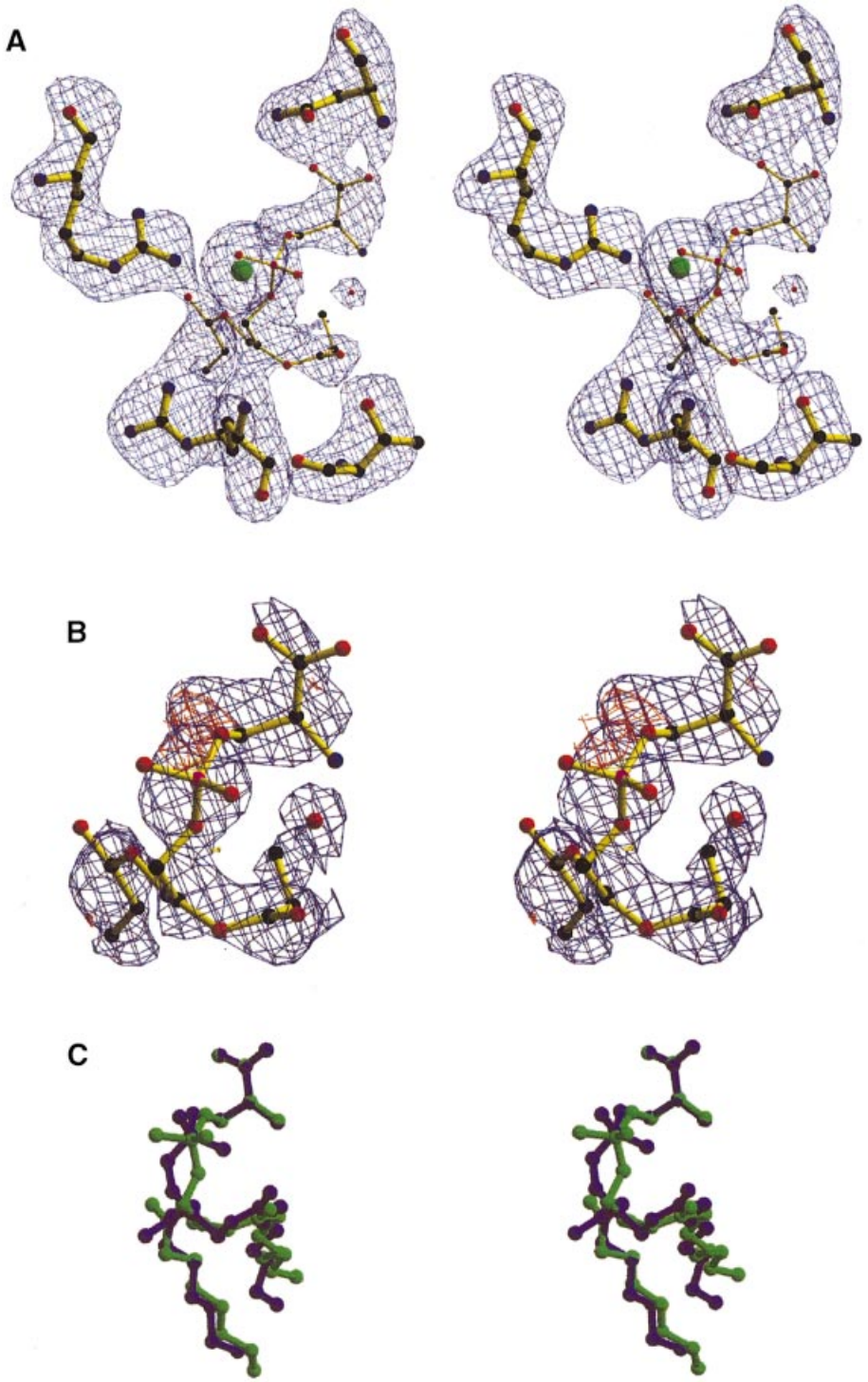

Fig. 3. (**A**) Stereoviews of the F_o–F_c omit map of the ternary complex at 2.6 Å resolution, in the vicinity of Ca1 contoured at 2σ. All the atoms corresponding to residues Asn189, Arg216, Arg249, Thr251 and also to the ion Ca1 and to the DCPS ligand were omitted for the map calculation according to the CNS protocols. The molecular fragments modeled into the corresponding density are also shown. The DCPS ligand is represented with the conformation corresponding to the *sn*-2 model (see the text). (**B**) Stereoviews, in the same orientation as in (A), of the F_o–F_c omit map (blue) of the ternary complex calculated omitting only the DCPS ligand. The residual F_o–F_c map calculated from the final refined model is also shown superimposed together with the DCPS model. Only some positive density (red) could be seen close to the position corresponding to the phosphoryl moiety. All the map contouring shown was carried out 2.5σ. (**C**) The superimposition of the two alternative DCPS conformations (*sn*-1 in purple and *sn*-2 in green) emphasizes the similar atomic disposition.

Furthermore, titration of the fluorescence intensity of PKCα-C2 domain with DCPS was used to characterize the lipid binding to the protein domain at different Ca^{2+} concentrations (Bashford *et al.*, 1979; Surewicz and Epand, 1984). Results show that binding of DCPS to the protein increases with the Ca^{2+} concentration; maximal binding activity was observed when 100 μM Ca^{2+} was used, while at 200 μM EGTA, used as a control, no binding was

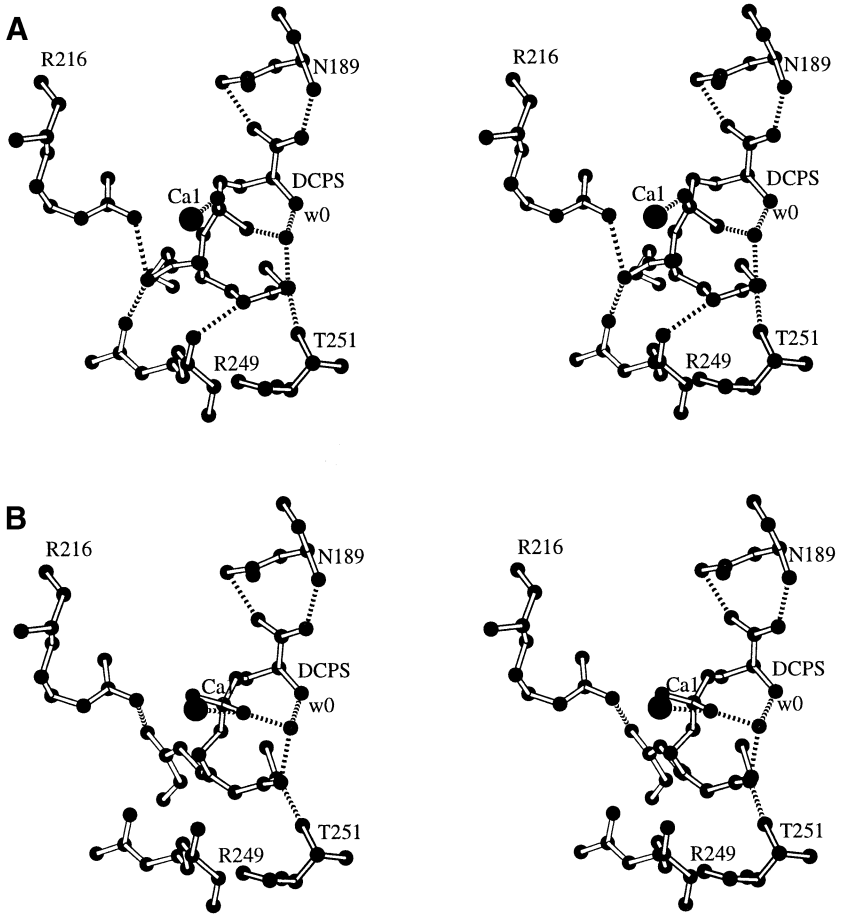

Fig. 4. Stereoview, with the same orientation as in Figure 3A, showing the interactions between DCPS, Ca1 and protein residues Asn189, Arg216, Arg249 and Thr251 for the *sn*-1 (**A**) and *sn*-2 (**B**) DCPS models. Possible hydrogen bonds and the coordination with the Ca1 ion are represented as discontinuous lines. The coordination distances between the Ca1 ion and the closest oxygen of the DCPS ligand are 2.1 and 2.4 Å for the *sn-1* and *sn-2* models, respectively. The presence of the bonded water molecule w0 enhances the quasi-cyclic character of the glycerophosphoserine moiety of DCPS.

detected (Figure 5A). These results would fully agree with a Ca^{2+}-dependent binding of DCPS to the PKCα-C2 domain, even allowing estimations of the apparent association constants (K_{app}) at different Ca^{2+} concentrations (Figure 5B), suggesting that the overall affinity of DCPS to the domain increases with Ca^{2+} concentration at ranges comprising 0.1 and 10 μM, and this is similar to those described for many C2 domains (Dafletov and Südhof, 1993; Nalefski *et al*., 1997; Corbalan-Garcia *et al*., 1999).

Discussion

C2 domains are remarkable folding modules widely distributed among membrane binding proteins. The dominant structural feature of the C2 domains is an eight-stranded β-sandwich motif, which can bind multiple Ca^{2+} ions at the tip of the domain in a region formed by strand connections, mainly loops CBR1 and CBR3. In conventional PKCs the Ca^{2+} binding properties to the C2 domain have been well characterized, but the mechanism by which Ca^{2+} binding promotes the translocation of the C2 domain to lipid vesicles is still unclear. A hallmark of PKC's lipid regulation is the remarkable specificity for its lipid activators (Newton and Johnson, 1998). Extensive biochemical studies have established that PKCα is maximally activated by 1,2-*sn*-diacylglycerol and 1,2-*sn*-phosphatidyl-L-serine lipids both in detergent–lipid mixed micelles (Lee and Bell, 1989) and in model membranes (Bazzi and Nelsestuen, 1987). It has also been shown that DCPS can activate PKC at the same level as other longer chain PSs such as bovine brain PS or 1-palmitoyl-2-oleyl-*sn*-phosphatidylserine (Walker *et al*., 1990; J.Garcia-Garcia, S.Corbalan-Garcia and J.C.Gómez-Fernández, unpublished data). Furthermore, we have demonstrated in this paper that DCPS is able to bind to the PKCα-C2 domain in a calcium-dependent manner. Pioneer works by Lee and Bell (1989, 1992) proposed that specific molecular determinants on PKC might recognize PS stereospecifically as both the carboxyl and amino moieties of PS and the distance between the phosphate and carboxyl and amino groups are important to achieve full activation of PKC. However, other anionic phospholipids can replace PS with varying degrees of effectiveness (Lee and Bell, 1992; Toker *et al*., 1994; Mosior *et al*., 1996; Epand *et al*., 1998). Furthermore, recent results have also demonstrated that, in the presence of DAG, PKC increases its affinity for 1,2-*sn*-phosphatidyl-L-serine, which supports the idea that selectivity is not only determined by the net phospholipid charge, but mainly by structural complementarity (Newton and Keranen, 1994; Johnson *et al*., 1998).

A number of models have been suggested to explain the peculiarities of the interaction of the C2 domain from

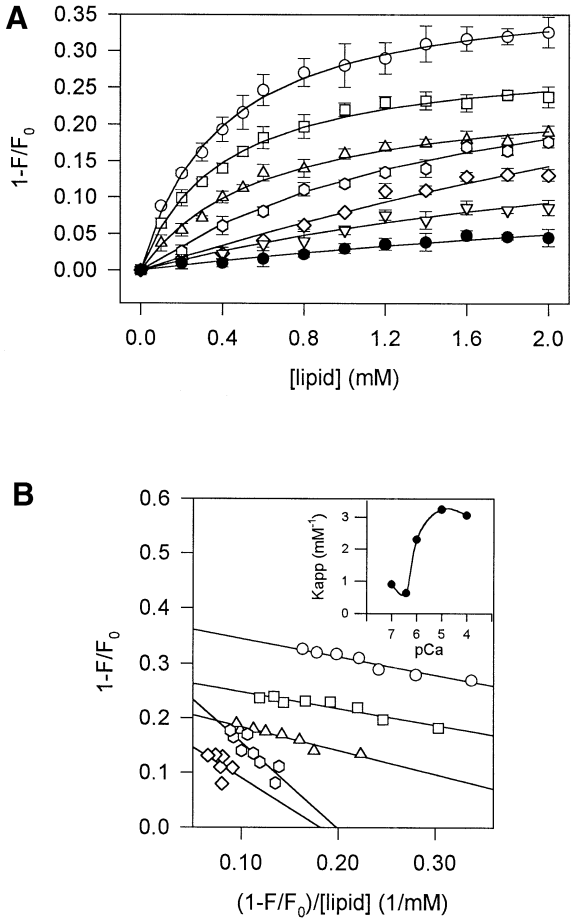

Fig. 5. Binding of DCPS to the PKCα-C2 domain. (**A**) DCPS binding to PKCα-C2 domain was measured at 100 (○), 10 (□), 1 (△), 0.34 (⬡), 0.1 (◇) and 0.02 (▽) μM $CaCl_2$ concentrations. EGTA (200 μM) was used as a control (●). The protein concentration was 0.5 μM and increasing concentrations of DCPS from 0.1 to 2 mM were added in each case. (**B**) Titration of the PKCα-C2 domain fluorescence with DCPS is plotted as $1 - F/F_0$ versus $(1 - F/F_0)$/[lipid], where F_0 and F are the fluorescence in the absence and presence of lipid, respectively. Straight lines indicate the initial slopes. The inset contains a schematic representation of K_{app} (mM^{-1}) versus the Ca^{2+} concentration, clearly showing that the overall affinity of DCPS for the protein is Ca^{2+}-dependent at concentrations close to 1 μM.

conventional PKCs with membranes. In a first model the altered surface potential, which would result from the Ca^{2+} binding, was proposed to act as an electrostatic switch mediating the macromolecular interactions of the C2 domain. However, mutational studies on conventional PKCs replacing aspartates by arginines in the calcium binding pocket, hence converting the negative electrostatic potential of the Ca^{2+} site to one that is electropositive, did not promote the binding of PKC to anionic membranes in the absence of Ca^{2+} (Edwards and Newton, 1997).

In a second model, the Ca^{2+} binding to the C2 domain was proposed to produce subtle rearrangements of positively charged side chains that would result in creating a lipid binding pocket not necessarily in the proximity of the Ca^{2+} ions. The co-crystallization of *o*-phospho-L-serine with the C2 domain of PKCβ showed some density in the vicinity of the lysine-rich cluster (Sutton and Sprang, 1998), and our data also indicate that phosphate groups can bind in this molecular area. However, extensive mutational studies on the PKC basic residues, mainly at the lysine-rich cluster and for residues Lys236/Lys238, had, at most, only minor effects on PKC calcium-dependent PS membrane binding and activity (Igarashi *et al*., 1995; Edwards and Newton, 1997; Johnson *et al*., 1997). Therefore, direct experimental evidence has still to be found for a calcium induction mechanism of a remote lipid pocket and even a role for the lysine-rich cluster during membrane binding remains questionable.

Results obtained in the present work, with the Ca1 ion directly coordinated to the phosphoryl oxygen of DCPS, suggest a third model that is reminiscent of those derived from the crystal structures of phospholipase A_2 and annexin V complexes, although a second Ca^{2+} ion also participates in substrate coordination for annexin (Scott *et al*., 1990, 1991; Swairjo *et al*., 1995). Direct bridging of the phospholipid to Ca^{2+} provides a structural explanation for most experimental observations about the reciprocal cooperativity observed when activating conventional PKCs. Thus, the higher affinity of PS when Ca^{2+} is present would be a direct consequence of the essential role of Ca^{2+} in the PS binding pocket. Subsequently, the interactions of the lipid with residues from the C2 domain would lock the bridging Ca^{2+} between the lipid and the protein, increasing the apparent affinity of C2 towards the calcium ion (Shao *et al*., 1996; Nalefski *et al*., 1997). The diversity and spatial disposition of the interactions observed in the PKCα-C2–Ca^{2+}–DCPS complex provide a rationale for the observed lipid specificity of conventional PKCs (Johnson *et al*., 1998) and might also explain some of the difficulties in finding soluble PS analogs suitable for high resolution structural studies. Thus, phospholipid analogs, such as *o*-phospho-L-serine or 3-glycero-*o*-phospho-L-serine, used to analyze the binding of phospholipids to PKCβ and annexin, respectively, lack the possibility of some of the interactions seen in the structure of the PKCα-C2–Ca^{2+}–DCPS complex (Swairjo *et al*., 1995; Sutton and Sprang, 1998). The different role of the two calcium ions, where only Ca1 is directly involved in bridging the C2 domain to the phospholipid, appears to correlate with mutagenesis studies of PKCα, and in this way substitutions by Asn of residues Asp187 and Asp193, which coordinate to Ca1 and are located in CBR1, have remarkably more significant effects on the vesicle binding than the mutations of residues Asp248 and Asp254, which coordinate to Ca2 and are located in CBR3 (Medkova and Cho, 1998).

Mutational studies on PKCα had shown that penetration of the C2 domain into PS-containing membranes was part of the changes required for PKCα activation and also essential for its interaction with DAG (Medkova and Cho, 1998). Double-site mutants Arg249/Arg252 and Trp245/Trp247 indicate that those arginines are involved in non-specific electrostatic interactions with the anionic membranes, whereas the tryptophans have hydrophobic interactions with the internal part of the membranes (Medkova and Cho, 1998; Bittova *et al*., 1999). The presence of the DCPS ligand in the PKCα-C2–Ca^{2+}–DCPS structure defines an approximate rigid body superimposition of the complex onto a membrane (Figure 6). In the resulting docked model most of the C2 domain remains in the cytosol with only the central part of CBR3, particularly side chains from residues Trp247 and Arg249, inserted into the lipid bilayer. In this model, the β3–β4

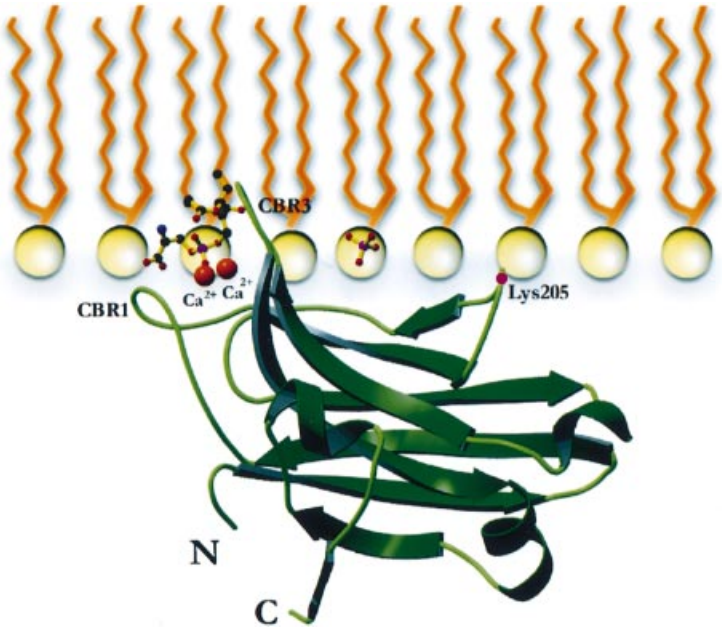

Fig. 6. Docking of the PKCα-C2–Ca^{2+}–DCPS ternary complex onto a model membrane as defined by the approximate superimposition of the DCPS structure onto an anionic lipid. In the resulting docked model only the central part of CBR3 from the C2 domain is inserted into the lipid bilayer, while the phosphate ion, found at the lysine-rich cluster region, might correspond to the polar head of another lipid molecule. In this model, the N and C ends of the C2 domain are both situated in the protein face opposite to the membrane.

connection of the C2 domain approaches the membrane surface, especially residue Lys205, without penetrating, and the phosphate molecule found at the lysine-rich cluster superimposes with a polar head from one of the membrane lipids. In this model, the N and C ends of the C2 domain are both situated in the protein face opposite to the membrane.

As a consequence of the structural and binding information described above, this work suggests a membrane binding mechanism of the PKCα-C2 domain in which Ca1 and Ca2 play different roles in membrane binding. These studies have also identified several residues that are directly involved in electrostatic and hydrophobic interactions with PS. We propose a two-step mechanism of function of the C2 domain as a membrane docking module in which Ca1 will trigger the interaction with negatively charged phospholipids at the membrane surface, and this first contact would enable different protein residues located in CRB3 to interact with the phospholipid, leading to membrane penetration. This model provides good insight into the PKCα membrane association process, which is the event that triggers the catalytic activation of the enzyme. These studies also support a better understanding of the mechanism of Ca^{2+}-dependent phospholipid binding that could be extended to other C2-domain-containing proteins.

Materials and methods

Expression plasmids

The DNA fragment corresponding to the C2 domain of PKCα (residues 155–293) was amplified using PCR with oligonucleotides 5PS and 3PS (sequences: 5′-CAAGAATTCACACAGAGAAGAGG-3′ and 5′-CAAAAGCTTTCATCCTTCTGGAATGGG-3′, respectively). PKCα cDNA was a kind gift from Drs Nishizuka and Ono (Kobe University, Kobe, Japan). The resulting 414 bp PCR fragment was subcloned into the *Eco*RI and *Hin*dIII sites of the bacterial expression vector pET28c(+) (Novagen), in which the insert is fused to a His_6 tag.

Expression and purification of the His-PKC-C2 domain

The pET28c(+) plasmid containing the PKC-C2 domain was transformed into BL21(DE3) *Escherichia coli* cells. The bacterial cultures (OD_{600} = 0.6) were induced for 5 h at 30°C with 0.5 mM isopropyl-β-D-thiogalactopyranoside (IPTG) (Boehringer Mannheim, Germany). The cells were lysed by sonication in lysis buffer (25 mM HEPES pH 7.4, 100 mM NaCl) containing protease inhibitors (10 mM benzamidine, 1 mM PMSF and 10 μg/ml trypsin inhibitor). The soluble fraction of the lysate was incubated with Ni–NTA agarose (Qiagen, Hilden, Germany) for 2 h at 4°C. The Ni beads were washed with lysis buffer containing 20 mM imidazole. The bound fractions were eluted with the same buffer containing 250 mM imidazole. His_6 tags were removed after thrombin cleavage, and finally the PKC-C2 domain was desalted and concentrated using an Ultrafree-5 centrifugal filter unit (Millipore Inc., Bedford, MA).

Binding of DCPS to the PKC-C2 domain

Steady-state fluorescence emission spectra were measured at 25°C in a Shimadzu RF-540 spectrofluorophotometer. The excitation wavelength was 280 nm and the emission wavelength ranged from 300 to 450 nm, the maximum was at 340 nm. Protein (0.5 μM) was dissolved in a buffer containing 100 mM NaCl, 20 mM HEPES pH 7.4 and different Ca^{2+} concentrations as indicated in Figure 5. Free Ca^{2+} concentration was estimated from total Ca^{2+} and EGTA concentrations (Fabiato, 1988). Contaminating Ca^{2+} in the buffer solution was determined by using a dual wavelength spectrophotometer (Bio-Logic Co., Claix, France) as described by Dani *et al.* (1979). Aliquots of a DCPS solution were added to the quartz cuvette containing the protein solution, and titration of the fluorescence intensity with DCPS was evaluated and used to determine the binding parameters (Bashford *et al*., 1979; Surewicz and Epand, 1984; Butko *et al*., 1997). This approach does not attempt to separate the association constant and stoichiometry, but it yields an overall affinity of the lipid to the protein. The ratio K_d/n of the dissociation constant and stoichiometry is the reciprocal of the classic first association constant K_{app} for the protein–lipid interaction. Provided that $C_L \gg C_P$ (C_L, DCPS concentration; C_P, protein concentration), K_d/n can be determined from the slope of the plot of $1 - F/F_0$ versus $(1 - F/F_0)/C_L$, where F_0 is fluorescence in the absence of quencher and F is fluorescence in the presence of quencher at a given concentration of DCPS. In this case, only the high-lipid-concentration data were taken into account to calculate K_{app}, since the low-lipid-concentration data do not fulfill the condition $C_L \gg C_P$ and consequently the model is not applicable.

Crystallization and data collection

Crystals of the calcium-bound form of the PKCα-C2 domain, both in the absence and presence of DCPS, were obtained with the hanging drop vapor diffusion technique at 20°C. Protein (4–8 mg/ml) was first incubated overnight at 4°C with 25 mM calcium chloride and 2 mM DCPS–25 mM $CaCl_2$, respectively.

Two milliliters of the protein complex were mixed with an equal volume of the crystallization buffer (20% PEG8K and 50 mM potassium phosphate pH 6.5) on silanized glass coverslips and inverted over a 1 ml reservoir containing the crystallization buffer. Crystals appeared after 3–4 days and grew slowly over 3 weeks to ~0.6 × 0.1 × 0.1 mm^3. Isomorphous crystals from PKCα-C2–Ca^{2+} and PKCα-C2–Ca^{2+}–DCPS had $P3_221$ symmetry with cell parameters a = 58.9, c = 91.3 Å (Table I), and contained one protein complex per asymmetric unit that would correspond to a specific volume solvent content of 50%. The PKCα-C2–Ca^{2+} data set was collected at 100 K by means of the cryo-crystallographic techniques using the crystallization buffer as a cryoprotectant. A 2.4 Å data set was measured from a single crystal using synchrotron radiation at the X31 beamline of the DESY Hamburg outstation on a Mar Research Imaging Plate using radiation of wavelength 0.91 Å. Diffraction intensities were indexed and integrated using the package Denzo and internally scaled with Scalepack (Otwinowski *et al*., 1996). The data were 96% complete at 2.4 Å resolution giving an internal agreement factor of 5% and an average $I/\sigma(I)$ of 10 for all reflections and 7 for the highest resolution shell (Table I). The X-ray data of the PKCα-C2–Ca^{2+}–DCPS complex were collected at room temperature with a Mar Research Imaging Plate in a Rigaku rotating anode generator and were reduced with the Denzo/Scalepack software. Data were 98% complete at 2.6 Å resolution (R_{symm} = 9%) and the $I/\sigma(I)$ in the last resolution shell was 5 (Table I).

Structure resolution and refinement

Both structures were determined by molecular replacement. The PKCα-C2–Ca^{2+} was solved and refined first, and then the final model obtained was used to refine the PKCα-C2–Ca^{2+}–DCPS complex. The C2–Ca^{2+} structure was determined using the AMoRe package (Navaza, 1994). The starting model was taken from the structure of the C2 domain of PKCβ (Sutton and Sprang, 1998; Protein Data Bank ID code 1A25) excluding Ca^{2+}, ligand and solvent molecules. The correctly oriented and positioned model yielded a correlation coeficient of 0.7 and an R-factor of 35% for data between 15 and 4 Å resolution.

Refinement was carried out following standard protocols using the CNS program iteratively (Brünger *et al*., 1998) with the amplitude based, maximum likelihood target function and alternating with manual rebuilding in the interactive graphics programs O and TURBO (Jones *et al*., 1991; Roussel and Cambillau, 1991). Bulk solvent correction and restrained, isotropic individual B-factors were used at the final rounds of refinement and model building. The refined atomic model for PKCα-C2–Ca^{2+} comprises 126 protein residues, 76 well ordered water molecules and two Ca^{2+} ions clearly discerned in the $2F_o$–F_c and F_o–F_c electron density maps. In addition, two phosphate ions were located in the structure. The first one was found coordinated with one of the Ca^{2+} ions (Figure 2B) and the second was located near a cluster of lysine residues in an equivalent position to that of a molecule of *o*-phospho-L-serine observed in the structure of the C2 domain of PKCβ (Sutton and Sprang, 1998). Both phosphate ions were included in the final model with a refined occupancy of 0.6 and 0.45, respectively. The R_{free} and R_{work} for the refined model were 0.27 and 0.22, respectively, for 6800 reflections with $F > 2\sigma F$ in the 18–2.4 shell (Table I).

To obtain an accurate model of the PKCα-C2–Ca^{2+}–DCPS complex, the coordinates of the PKCα-C2–Ca^{2+} model were subjected to a crystallographic refinement against structure factor amplitudes measured from crystals of the DCPS complex (F_{oDCPS}); the solvent molecules and ions were not included in this model. The F_o–F_c difference map showed two clear peaks at the putative Ca^{2+} binding sites and a continuous density with a nearly cyclic shape that would correspond to one molecule of DCPS closely connected with one of the Ca^{2+} ions. The conformation of the glycerophosphoserine head group, as seen in the complex with annexin V (Swairjo *et al*., 1995), was used to start the modeling of the DCPS structure, while the two acyl chains were manually built with correct bond distances and angles using programs O and TURBO (Jones *et al*., 1991; Roussel and Cambillau, 1991). Two possible interactions between the amino group of the phosphoserine moiety contacting with the fatty acyl ester carbonyl groups *sn*-1 or *sn*-2, explained the quasi-cyclic density almost equally well. Protein–ligand interactions were also similar for both models (Figure 4). However, the model involving interactions with the carbonyl group *sn*-1 showed consistently better agreement factors in the refinement and was considered to be the most probable model (Table I).

The $2F_o$–F_c electron density maps showed weak electron density for the DCPS, probably due to the partial occupancy of this bound ligand. The partial occupancy observed for the lipid ligand was refined with the program CNS to 0.55. Final cycles of Powell minimization of potential energy terms gave R_{free} and R_{work} values of 23.3 and 19.5%, respectively, for 5432 reflections with $F > 2\sigma F$ for data between 20 and 2.6 Å. The refined atomic model of the PKCα-C2–Ca^{2+}–DCPS comprises 126 protein residues, 38 well ordered water molecules, two Ca^{2+} ions, one phosphate ion and one DCPS ligand molecule (Table I).

The deviation from ideal geometry of the PKCα-C2 models was analyzed using the program PROCHECK (Laskowski *et al*., 1993). Eighty-five percent of the non-glycine residues fall within the most favored regions of the Ramachandran plot and the rest are inside the 'additional allowed regions'. The stereochemistry of both the Ca^{2+} and Ca^{2+}–DCPS models is given in Table I. The comparisons between the different C2 models were made using the program SHP.

Cooordinates of both DCPS-bound and unbound structures will be deposited in the Protein Data Bank, and are available directly from the authors on request until they have been processed and released.

Acknowledgements

We wish to thank Drs Ono and Nishizuka for the kind gift of the cDNA coding for PKCα. Research at the IBMB-CSIC was supported by grant PB95-0218 from DGES (Spain). Work at the Universidad de Murcia was supported by grants PB95-1022 and PB96-1107 from DGES (Spain). W.F.O. is a recipient of a fellowship from the MEC.

References

Bashford,C.L., Chance,B., Smith,J.C. and Yoshida,T. (1979) The behaviour of oxonol dyes in phospholipid dispersions. *Biophys. J.*, **25**, 63–85.

Basu,A. (1993) The potential of protein kinase C as a target for anticancer treatment. *Pharmacol. Ther.*, **59**, 257–280.

Bazzi,M.D. and Nelsestuen,G.L. (1987) Association of protein kinase C with phospholipid vesicles. *Biochemistry*, **26**, 115–122.

Bazzi,M.D. and Nelsestuen,G.L. (1990) Protein kinase C interaction with calcium: a phospholipid-dependent process. *Biochemistry*, **29**, 7624–7630.

Bittova,L., Sumandea,M. and Cho,W. (1999) A structure–function study of the C2 domain of cytosolic phospholipase A_2. *J. Biol. Chem.*, **274**, 9665–9672.

Boni,L.T. and Rando,R.R. (1985) The nature of protein kinase C activation by physically defined phospholipid vesicles and diacylglycerols. *J. Biol. Chem.*, **260**, 10819–10825.

Brünger,A.T. *et al.* (1998) Crystallography and NMR system: a new software suite for macromolecular structure determination. *Acta Crystallogr. D Biol. Crystallogr.*, **54**, 905–921.

Butko,P., Huang,D., Pustai-Carey,M. and Surewicz,W.K. (1997) Interaction of the δ-endotoxin CytA from *Bacillus thuringiensis* var. *israelensis* with lipid membranes. *Biochemistry*, **36**, 12862–12868.

Corbalan-Garcia,S., Rodriguez-Alfaro,J.A. and Gómez-Fernández,J.C. (1999) Determination of the calcium-binding sites of the C2 domain of protein kinase Cα that are critical for its translocation to the plasma membrane. *Biochem. J.*, **337**, 513–521.

Coussens,L., Parker,P.J., Rhee,L., Yang-Feng,T.L., Chen,E., Waterfield,M.D., Francke,U. and Ullrich,A. (1986) Multiple, distinct forms of bovine and human protein kinase C suggest diversity in cellular signaling pathways. *Science*, **233**, 859–866.

Davletov,B.A. and Südhof,T.C. (1993) A single C2 domain from synaptotagmin I is sufficient for high affinity Ca^{2+}/phospholipid binding. *J. Biol. Chem.*, **268**, 26386–26390.

Dekker,L.V. and Parker,P.J. (1994) Protein kinase C—a question of specificity. *Trends Biochem. Sci.*, **19**, 73–77.

Dessen,A., Tang,J., Schmidt,H., Stahl,M., Clark,J.D., Seehra,J. and Somers,W.S. (1999) Crystal structure of human cytosolic phospholipase A_2 reveals a novel topology and catalytic mechanism. *Cell*, **97**, 349–360.

Edwards,A.S. and Newton,A.C. (1997) Regulation of protein kinase C βII by its C2 domain. *Biochemistry*, **36**, 15615–15623.

Epand,R.M., Stevenson,C., Bruins,R., Schram,V. and Glaser,M. (1998) The chirality of phosphatidylserine and the activation of protein kinase C. *Biochemistry*, **37**, 12068–12073.

Essen,L.-O., Perisic,O., Cheung,R., Katan,M. and Williams,R.L. (1996) Crystal structure of a mammalian phosphoinositide-specific phospholipase Cδ. *Nature*, **380**, 595–602.

Essen,L.-O., Perisic,O., Lynch,D.E., Katan,M. and Williams,R.L. (1997) A ternary metal binding site in the C2 domain of phosphoinositide-specific phospholipase C-δ1. *Biochemistry*, **36**, 2753–2762.

Fabiato,A. (1988) Computer programs for calculating total from specified free or free from specified total ionic concentrations in aqueous solutions containing multiple metals and ligands. *Methods Enzymol.*, **157**, 378–417.

Igarashi,K., Kaneda,M., Yamaji,A., Saido,T.C., Kikkawa,U., Ono,U., Inoue,K. and Umeda,M. (1995) A novel phosphatidylserine-binding peptide motif defined by an anti-idiotypic monoclonal antibody. Localization of phosphatidylserine-specific binding sites on protein kinase C and phosphatidylserine decarboxylase. *J. Biol. Chem.*, **270**, 29075–29078.

Johnson,J.E., Edwards,A.S. and Newton,A.C. (1997) A putative phosphatidylserine binding motif is not involved in the lipid regulation of protein kinase C. *J. Biol. Chem.*, **272**, 30787–30792.

Johnson,J.E., Zimmerman,M.L., Daleke,D.L. and Newton,A.C. (1998) Lipid structure and not membrane structure is the major determinant in the regulation of protein kinase C by phosphatidylserine. *Biochemistry*, **37**, 12020–12025.

Jones,T.A., Zou,J.Y., Cowan,S.W. and Kjeldgaard,M. (1991) Improved methods for building protein models in electron density maps and the location of errors in these models *Acta Crystallogr. A*, **47**, 110–119.

Laskowski,R.A., MacArthur,M.W., Moss,D.S. and Thornton,J.M. (1993) PROCHECK: a program to check the stereochemical quality of protein structures. *J. Appl. Crystallogr.*, **26**, 283–291.

Lee,M.-H. and Bell,R.M. (1989) Phospholipid functional groups involved in protein kinase C activation, phorbol ester binding and binding to mixed micelles. *J. Biol. Chem.*, **264**, 14797–14805.

Lee,M.-H. and Bell,R.M. (1992) Supplementation of the phosphatidyl-L-serine requirement of protein kinase C with nonactivating phospholipids. *Biochemistry*, **31**, 5176–5182.

Medkova,M. and Cho,W. (1998) Mutagenesis of the C2 domain of protein kinase Cα. *J. Biol. Chem.*, **273**, 17544–17552.

Mellor,H. and Parker,P.J. (1998) The extended protein kinase C superfamily. *Biochem. J.*, **332**, 281–292.

Mosior,M., Golini,E.S. and Epand,R.M. (1996) Chemical specificity and physical properties of the lipid bilayer in the regulation of protein kinase C by anionic phospholipids: evidence for the lack of a specific binding site for phosphatidylserine. *Proc. Natl Acad. Sci. USA*, **93**, 1907–1912.

Nalefski,E.A. and Falke,J.J. (1996) The C2 domain calcium-binding motif: structural and functional diversity. *Protein Sci.*, **5**, 2375–2390.

Nalefski,E.A., Slazas,M.M. and Falke,J.J. (1997) Calcium signaling cycle of a membrane-docking C2 domain. *Biochemistry*, **36**, 12011–12018.

Navaza,J. (1994) AMoRe: an automated package for molecular replacement. *Acta Crystallogr. A*, **50**, 157–163.

Newton,A. (1995) Protein kinase C: structure, function and regulation. *J. Biol. Chem.*, **270**, 28495–28498.

Newton,A. and Johnson,J.E. (1998) Protein kinase C: a paradigm for regulation of protein function by two membrane-targeting modules. *Biochim. Biophys. Acta*, **1376**, 155–172.

Newton,A.C. and Keranen,L.M. (1994) Phosphatidyl-L-serine is necessary for protein kinase C's high-affinity interaction with diacylglycerol-containing membranes. *Biochemistry*, **33**, 6651–6658.

Nicholls,A., Sharp,K. and Honig,B. (1991) GRASP, graphical representation and analysis of structural properties of proteins. *Proteins*, **11**, 281–296.

Nishizuka,Y. (1995) Protein kinase C and lipid signaling for sustained cellular responses. *FASEB J.*, **9**, 484–496.

Otwinowski,Z. and Minor,W. (1996) Processing of X-ray diffraction data collected in an oscillation mode. *Methods Enzymol.*, **276**, 307–326.

Pappa,H., Murray-Rust,J., Dekker,L.V., Parker,P.J. and McDonald,N.Q. (1998) Crystal structure of the C2 domain from protein kinase Cδ. *Structure*, **6**, 885–894.

Perisic,O., Fong,S., Lynch,D.E., Bycroft,M. and Williams,R.L. (1998) Crystal structure of a calcium-phospholipid binding domain from cytosolic phospholipase A_2. *J. Biol. Chem.*, **273**, 1596–1604.

Rizo,J. and Südhof,T.C. (1998) C2-domains, structure and function of a universal Ca^{2+}-binding domain. *J. Biol. Chem.*, **273**, 15879–15882.

Roussel,A. and Cambillau,C. (1991) *TURBO Manual*. Silicon Graphics, Mountain View, CA.

Scott,D.L., White,S.P., Otwinowski,Z., Yuan,W., Gelb,M.H. and Sigler,P.B. (1990) Interfacial catalysis: the mechanism of phospholipase A_2. *Science*, **250**, 1541–1546.

Scott,D.L., White,S.P., Browning,J.L., Rosa,J.J., Gelb,M.H. and Sigler,P.B. (1991) Structures of free and inhibited human secretory phospholipase A_2 from inflammatory exudate. *Science*, **254**, 1007–1010.

Shao,X., Davletov,B.A., Sutton,R.B., Südhof,T.C. and Rizo,J. (1996) Bipartite Ca^{2+} binding motif in C2 domains of synaptotagmin and PKC. *Science*, **273**, 248–251.

Surewicz,W.K. and Epand,R.M. (1984) Role of peptide structure in lipid–peptide interactions: a fluorescence study of the binding of pentagastrin-related pentapeptides to phospholipid vesicles. *Biochemistry*, **23**, 6072–6077.

Sutton,R.B. and Sprang,S.R. (1998) Structure of the protein kinase Cβ phospholipid-binding C2 domain complexed with Ca^{2+}. *Structure*, **6**, 1395–1405.

Sutton,R.B., Davletov,B.A., Berghuis,A.M., Südhof,T.C. and Sprang,S.R. (1995) Structure of the first C2 domain of synaptotagmin I: a novel calcium/phospholipid-binding fold. *Cell*, **80**, 929–938.

Swairjo,M.A., Concha,N.O., Kaltzel,M.A., Dedman,J. and Seaton,B.A. (1995) Calcium-bridging mechanism and phospholipid head group recognition in the membrane-binding protein annexin V. *Nature Struct. Biol.*, **2**, 968–974.

Toker,A., Meyer,M., Reddy,K.K., Falck,J.R., Aneja,S., Parra,A., Burns,D.J., Ballas,L.M. and Cantley,L.C. (1994) Activation of protein kinase C family members by the novel polyphosphoinositides PtdIns-3,4-P2 and PtdIns-3,4,5-P3. *J. Biol. Chem.*, **269**, 32358–32367.

Walker,J.M., Homan,E.C. and Sando,J.J. (1990) Differential activation of protein kinase C isozymes by short chain phosphatidylserines and phosphatidylcholines. *J. Biol. Chem.*, **265**, 8016–8021.

Received July 8, 1999; revised and accepted September 21, 1999